REVISTA BRASILEIRA DE CIENCIAS MECANICAS
JOURNAL OF THE BRAZILIAN SOCIETY OF MECHANICAL SCIENCES

REVISTA BRASILEIRA DE CIÊNCIAS MECÂNICAS
JOURNAL OF THE BRAZILIAN SOCIETY OF MECHANICAL SCIENCES
Vol. 1. Nº 1 (1979) -
Rio de Janeiro: Associação Brasileira de Ciências Mecânicas
Trimestral
Inclui referências bibliográficas.
1. Mecânica
ISSN-0100-7386

A REVISTA BRASILEIRA DE CIÊNCIAS MECÂNICAS publica trabalhos que cobrem os vários aspectos da ciência e da tecnologia em Engenharia Mecânica, incluindo interfaces com as Engenharias Civil, Elétrica, Química, Naval, Nuclear, Aeroespacial, Alimentos, Agrícola, Petróleo, Materiais, etc., bem como aplicações da Física e da Matemática à Mecânica.

Publicação da /Published by
ASSOCIAÇÃO BRASILEIRA DE CIÊNCIAS MECÂNICAS-
THE BRAZILIAN SOCIETY OF MECHANICAL SCIENCES

Secretária da ABCM: Ana Lucia Fróes de Souza
Av. Rio Branco, 124-18º andar - Rio de Janeiro - Brasil
Tel. / Fax (021) 222-7128

Presidente: Arthur Palmeira Ripper
Vice-Presidente: Sidney Stuckenbruk
Secret. Geral: Agamenon R. E. Oliveira
Secretário: Carlos Alberto de Almeida
Diretor de Patrimônio: Luiz Fernando Salgado Candiota

REVISTA FINANCIADA COM RECURSOS DO
Programa de Apoio a Publicações Científicas
MCT CNPq FINEP
FAPESP - Fundação de Amparo a Pesquisa do Estado de São Paulo

RBCM - J. of the Braz. Soc. Mechanical Sciences
Vol. XV - nº 1 - 1993 - pp. 1-20
ISSN 0100-7386
Printed in Brazil

Chaotic Vibrations of an Oscillator with Shape Memory

Vibrações Caóticas de um Oscilador com Memória de Forma

Marcelo A. Savi
Arthur M. B. Braga
Departamento de Engenharia Mecânica
Pontifícia Universidade Católica do Rio de Janeiro
22453 Rio de Janeiro, RJ - Brasil

Abstract

This article reports results from some investigation on the dynamical behavior of mechanical systems containing elements with shape memory. some phenomenological theories that describe shape memory and pseudoelastic effects in metallic alloys that undergo thermoelastic martensitic transformations are reviewed. One of these theories is used to model a helical spring. The dynamic response of an oscillator with a shape memory spring is investigated. It is shown that the system may behave chaotically under certain conditions.
Keywords: Chaotic Vibrations - Nonlinear Dynamics - Shape Memory

Resumo

Este trabalho apresenta resultados de um estudo sobre a resposta dinâmica de sistemas mecânicos contendo elementos com memória de forma. São discutidas algumas teorias fenomenológicas que descrevem os efeitos de memória de forma e pseudoelasticidade associados a transformações martensíticas termoelásticas em ligas metálicas. Uma destas teorias é utilizada na modelagem de uma mola helicoidal. O comportamento dinâmico de um oscilador com memória de forma é investigado. Verifica-se que o sistema pode responder caoticamente sob determinadas condições.
Palavras-chave: Vibrações Caóticas - Dinâmica Não-Linear - Memória de Forma

Introduction

Shape memory and stress-induced pseudoelasticity are effects observed in metallic alloys that undergo thermoelastic martensitic transformations (see, e.g., Buehler et al., 1963; Jackson et al., 1972; Delaey et al., 1974; Warlimont et al., 1974; Schetky, 1979). Qualitative plots in Fig. 1 illustrate both behaviors. The stress-strain curve in Fig. 1a is obtained at constant temperature, and shows the

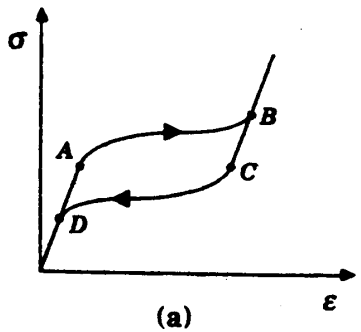

(a)

Fig. 1a. The pseudoelastic effect

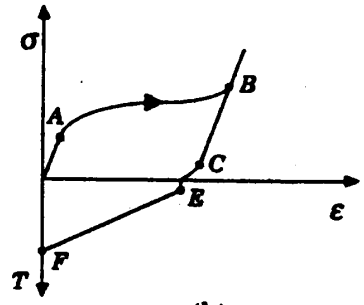

(b)

Fig 1b. The shape memory effect

Manuscript received December 1992. Associate Technical Editor: Agenor de Toledo Fleury

pseudoelastic strain recovery during a loading-unloading cycle. This behavior is typical at a temperature where the parent phase, austenite, is stable. At the point A in the diagram, the stress-induced transformation starts to cause the appearance of martensite. This process is completed at B, and the now all martensitic specimen deforms elastically again. During unloading, the transformation is reversed in the path CD, and the sample returns to its undeformed austenitic state.

The plot in Fig. 1b is obtained at a different temperature. The reverse transformation is not completed after the load is removed, and some permanent strain is still observed in the stress-free specimen. The shape memory effect consists in the recovery of this residual deformation by heating the sample to a temperature where the parent phase is stable. The temperature-induced reverse transformation occurs in the segment EF of the diagram.

The shape memory effect and other related thermoelastic processes associated with martensitic transformations have been known since at least 1938. But it has been the investigations of Buehler and co-workers (see, e.g., Buehler et al., 1963) on phase changes in NiTi alloys, in the early sixties, that instigated the technological interest in the shape memory effect. Experiments where NiTi objects were restored to their original shape after being "permanently" deformed, revealed the potential for the use of these alloys in engineering (Jackson et al., 1972; Schetky, 1979). Among other applications, one could mention self-actuating fasteners, self-erectable structures for aerospace hardware, thermally actuated switches, and a number of bioengineering devices. Most recently, shape memory alloys have also been employed as actuators for the active vibration control of flexible structures (Rogers, 1990; Rogers et al., 1991; Venkatesh et al., 1992).

The phenomena associated with martensitic transformations are intrinsically nonlinear. As a consequence, when subjected to dynamic inputs, a mechanical system which contains shape memory elements may experience a number of quite complex behaviors. One of them is chaos.

Chaotic response is characterized by long term unpredictability. A nonlinear system which is deterministic may experience completely irregular behavior even when excited periodically. This apparently random response has nevertheless a structure. The study of the structure underlying chaos has been a very active field in recent years. We refer to the books by Thompson and Stewart (1986) and Moon (1987) for lists of publications on the subject.

In this paper we are concerned with the chaotic response of mechanical system with shape memory. Firstly, we briefly review some of the available phenomenological theories that describe thermoelastic martensitic transformations in metallic alloys. One of these theories is used to build a model of an helical spring with shape memory. The dynamics of a simple, one degree-of-freedom oscillator is then investigated.

Phenomenological Theories for Shape Memory

Shape memory and other related effects associated with thermoelastic martensitic transformations may be modeled at either the microscopic or macroscopic levels. For descriptions at the microscopic level we refer to the articles by Achenbach and Müller (1982) and Warlimont et al. (1974). Here we are interested in phenomenological theories that describe the transformations macroscopically. These transformations are caused by changes in temperature as well as by mechanical actions. Hence, the macroscopic thermodynamical variables needed to describe the phenomena are temperature, T, and strain, ε. We consider small deformations only, in which case ε represents the infinitesimal strain tensor.

In order to account for the influence of phase transitions on the properties of shape memory alloys, there may also be a need for internal variables. The free energy, ψ, is then assumed to have the form

$$\psi = \psi(\varepsilon, T, \beta) \tag{1}$$

where β is a vector representing the internal variables.

If thermal dissipation is not considered, the Clausius-Duhem inequality may be written as (see, e.g., Germain, 1973)

$$\sigma : \dot{\varepsilon} - \rho(\dot{\psi} + s\dot{T}) \geq 0 \tag{2}$$

where ρ is the mass density, s the total entropy per unit of mass, and σ the Cauchy stress tensor.

From Eq. (1) one has

$$\dot{\psi} = \nabla_{\varepsilon}\psi : \dot{\varepsilon} + \nabla_{\beta}\psi \cdot \dot{\beta} + \frac{\partial \psi}{\partial T}\dot{T} \tag{3}$$

where $\nabla_{\varepsilon}\psi$ and $\nabla_{\beta}\psi$ represent the gradients of the free energy with respect to ε and β respectively. If we now define

$$\sigma = \rho \nabla_{\varepsilon}\psi \tag{4}$$

$$B = -\rho \nabla_{\beta}\psi \tag{5}$$

and assume that (Germain, 1973)

$$\frac{\partial \psi}{\partial T} = -s \tag{6}$$

the inequality (2) may be rewritten as

$$(\sigma - \bar{\sigma}) : \dot{\varepsilon} + B \cdot \dot{\beta} \geq 0 \tag{7}$$

If dissipation is not considered, Eq. (7) becomes an equality, otherwise we introduce a pseudo-potential of dissipation, $\phi(\dot{\varepsilon}, \dot{\beta})$, which is convex, positive, and vanishes at the origin. In this case, if we let

$$\sigma = \bar{\sigma}(\varepsilon, \beta, T) + \nabla_{\dot{\varepsilon}}\phi(\dot{\varepsilon}, \dot{\beta}) \tag{8}$$

and

$$B = \nabla_{\dot{\beta}}\phi(\dot{\varepsilon}, \dot{\beta}) \tag{9}$$

the Clausius-Duhen inequality is automatically satisfied (Germain, 1973).

Mathematical models for shape memory are based on different choices for the functionals representing the free energy and the pseudo-potential of dissipation. We now briefly review some of these models.

Model with Polynomial Free-Energy

The first model discussed here is based on Devonshire theory for temperature-induced first order phase transition combined with hysteresis, and has been proposed by Falk (1982). This is an one-dimensional model which does not consider dissipation. In Devonshire theory, the free energy depends on the temperature and on the one-dimensional strain ε, i.e.

$$\psi = \psi(\varepsilon, T) \tag{10}$$

and no internal variable is considered.

The functional form of the free energy is chosen such that at high temperatures it has only one minimum at vanishing strain, representing the equilibrium of the parent phase. At low temperatures, martensite is stable, and the free energy must have minima at nonvanishing strains. At intermediate temperatures the free energy must have equilibrium points corresponding to both phases. These restrictions are satisfied by the polynomial expression

$$\rho\psi(\varepsilon, T) = \frac{1}{2}a(T - T_M)\varepsilon^2 - \frac{1}{4}b\varepsilon^4 + \frac{1}{6}e\varepsilon^6 \tag{11}$$

where a, b, and e are positive constants, while T_M is the temperature below which the parent phase becomes unstable. It is also convenient to define the temperature T_A, above which austenite is stable, and the free-energy has only one minimum at zero strain,

$$T_A = T_M + \frac{1}{4}\frac{b^2}{ae} \tag{12}$$

Using expression (12) to eliminate e, and recalling that without dissipation the stress is simply the derivative of the free energy with respect to strain, we obtain the constitutive law based on Devonshire theory:

$$\sigma = a(T - T_M)\varepsilon - b\varepsilon^3 + \frac{1}{4}\frac{b^2}{a(T_A - T_M)}\varepsilon^5 \tag{13}$$

Stress-strain curves based on the polynomial model are shown in Fig. 2, where the thick lines

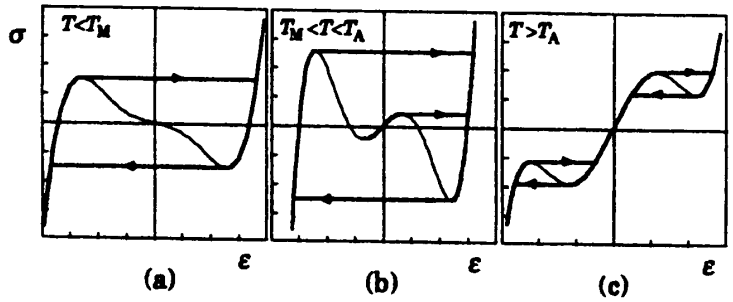

Fig. 2 Stress-Strain curves based on the polynomial model. Thick lines represent stable loading paths.

represent stable loading-unloading paths. The shape memory effect is illustrated in Fig. 2a and 2b, obtained for temperatures below T_A. The curve in Fig. 2c is representative of higher temperatures, and shows the pseudoelastic phenomenon described by the polynomial model.

Model with Assumed Transformation Kinetics

Another theory that models the one-dimensional mechanics of martensitic phase transformations has been developed by Tanaka and co-workers (Tanaka and Nagaki, 1982; Tanaka, 1985; Sato et al., 1985; Tobushi and Tanaka, 1990). In addition to uniaxial strain and temperature, Tanaka's theory also considers a scalar internal variable that characterizes the extent of transformation. This variable, β_1, represents the volumetric fraction of martensite. The free energy has the form

$$\psi = \psi(\varepsilon, \beta_1, T) \tag{14}$$

The constitutive equation may be written in rate form as

$$\dot{\sigma} = E\dot{\varepsilon} - \alpha\dot{\beta}_1 - \Xi\dot{T} \tag{15}$$

where

$$E = \rho\frac{\partial^2\psi}{\partial\varepsilon^2}, \quad \alpha = \rho\frac{\partial^2\psi}{\partial\varepsilon\partial\beta_1}, \quad \text{and} \quad \Xi = \rho\frac{\partial^2\psi}{\partial\varepsilon\partial T} \tag{16}$$

In Eq. (15), E is the elastic modulus and Ξ a thermoelastic coefficient, while α is associated with volume changes in the transformation (Sato et al., 1985). In general, these coefficients depend on the state variables ε, T, and β_1, but in the articles by Tanaka (1985), Sato et al. (1985), and Tobushi and Tanaka (1990), they are assumed to be constant and positive.

The other assumption in Tanaka's theory, is that the fraction of martensite is determined only through the current values of stress and temperature (Sato et al., 1985), i.e.

$$\beta_1 = B(\sigma, T) \tag{17}$$

The hypothesis is based on the difusionless nature of martensitic transformations (Tanaka, 1985). Sato et al. (1985) assume an exponential form for the functional on the right-hand-side of (17). The transformation from austenite to martensite is then described by

$$\beta_1 = 1 - \exp[-a_M(T_M - T) - b_M\sigma] \tag{18}$$

where T_M is the temperature where martensite starts to form under stress-free state, while a_M and b_M are positive constants (Sato et al., 1985). Eq. (18) holds for

$$\sigma \geq \left(\frac{a_M}{b_M}\right)(T - T_M) \tag{19}$$

The reverse transformation is described by another exponential function (Sato et al., 1985)

$$\beta_1 = \exp[-a_A(T - T_A) + b_A\sigma] \tag{20}$$

where a_A and b_A are positive constants while T_A is the temperature where austenite starts to form under zero stress. The kinetics of the reverse transformation (20) holds for

$$\sigma \leq \left(\frac{a_A}{b_A}\right)(T - T_A) \tag{21}$$

The dependency of martensite fraction on temperature under stress-free state, is schematically shown in Fig. 3a. The plot in Fig. 3b illustrates the kinetics of the stress induced transformation under constant temperature.

Tanaka's theory is capable of modeling the pseudoelastic behavior as well as the shape memory effect, and has been used in a number of applications (Sato et al., 1985; Tobushi and Tanaka, 1990). Rogers et al. (1991) and Liang and Rogers (1990) have employed a modification of this theory to develop a mathematical model for shape memory alloy hybrid composites used in structural acoustics control. In their model, instead of the exponential law presented above, the kinetics of transformation is described by a cosine function (Liang and Rogers, 1990). Results of Roger's model are in close agreement with experimental data (Rogers et al., 1989; Rogers, 1990).

It should be pointed out, however, that Tanaka's model, at least in the form presented above or in the references cited here, does only apply to tensile behavior. This is not explicitly stated by Sato et al. (1985). Furthermore, the stress-strain plot in compression presented in that article, Fig. 5 in (Sato et al., 1985), can not be obtained by applying only the set of equations introduced by its authors and repeated above. We believe that in order to correctly describe the shape memory alloy response under compressive loads, one has to introduce another internal variable, β_2, representing the volumetric fraction of a second variant of martensite. Of course, the following restriction must then be satisfied:

$$\beta_1 + \beta_2 \leq 1 \tag{22}$$

It is well known that shape memory alloys usually develop various kinds of martensite (Jackson et al., 1972; Delaey et al., 1974; Warlimont et al., 1974), and that in the same alloy, each variant grows favorably under one type of stress state (Schetky, 1979). Here, the second variant, β_2, should grow at the expense of β_1 under compressive loads and vice-versa. This and restriction (22), have to be taken into account in the assumptions concerning the transformation kinetics of the martensite variants.

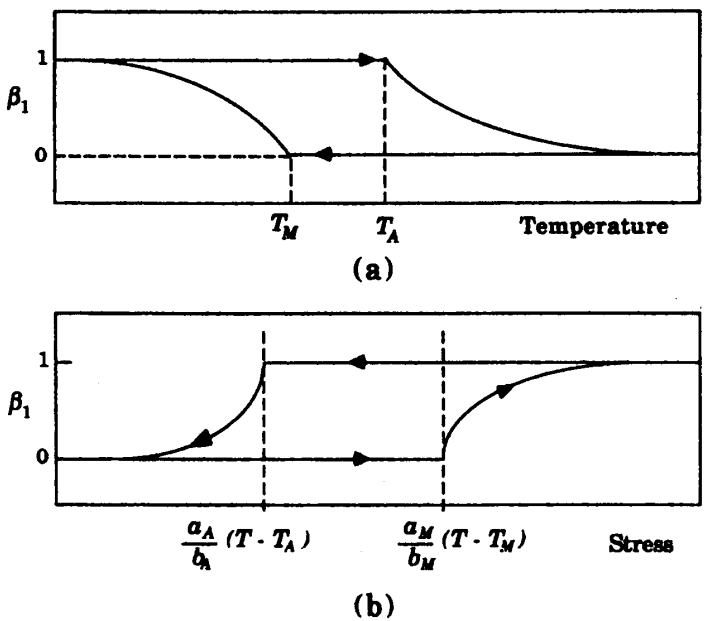

Fig. 3 Variation of martensite fraction with temperature at the stress-free state (a), and with stress under constant temperature (b).

Model with Internal Restrictions

The third type of phenomenological theory considered here has been developed by Fremond (1987). The shape memory and pseudoelastic effects are described with the aid of three internal variables, β_1, β_2, and β_3, respectively representing the volumetric fractions of two variants of martensite and of the austenitic parent phase. In this three-dimensional model, the three different phases may coexist, and the internal variables have to satisfy the following constraints:

$$0 \le \beta_i \le 1 \,(i = 1, 2, 3) \text{ and } \beta_1 + \beta_2 + \beta_3 = 1 \tag{23}$$

The free-energy of the mixture is then defined as

$$\rho\psi(\varepsilon, \beta_i, T) = \rho \sum_{i=1}^{3} \beta_i \psi_i(\varepsilon, T) + \bar{I}(\beta_i) \tag{24}$$

where $\psi_i(\varepsilon, T)$ is the free-energy of the individual phases and $\bar{I}(\beta_i)$ is the indicator function (Rockafellar, 1970) of the convex set

$$C = \{(\beta_1, \beta_2, \beta_3) \,|\, 0 \le \beta_i \le 1;\ \beta_1 + \beta_2 + \beta_3 = 1\} \tag{25}$$

and defined as

$$\bar{I}(\beta_i) = 0 \quad \text{if } \beta_i \in C$$

The functions describing the free-energy of the individual phases are chosen as

$$\begin{aligned}
\rho\psi_1(\varepsilon, T) &= \frac{1}{2}\varepsilon : \quad C : \varepsilon - \alpha(T)\,\mathrm{tr}(\varepsilon) \\
\rho\psi_2(\varepsilon, T) &= \frac{1}{2}\varepsilon : \quad C : \varepsilon + \alpha(T)\,\mathrm{tr}(\varepsilon) \\
\rho\psi_3(\varepsilon, T) &= \frac{1}{2}\varepsilon : \quad C : \varepsilon - \frac{L}{T_M}(T - T_M)
\end{aligned} \tag{27}$$

where C is the elasticity tensor, $\alpha(T)$ is proportional to the coefficient of thermal expansion, and L is the latent heat of the martensite-austenite phase change. Observe that all phases are assumed to have the same mass density and elastic properties. Also notice that since this is a three-dimensinal theory, in the previous equations ε represents the tensor of infinitesimal strains.

Using the second of equations (23), one can eliminate β_3 from the expression for the free-energy of the mixture, obtaining

$$\begin{aligned}
\rho\psi(\varepsilon, \beta_1, \beta_2, T) &= \rho\{\beta_1[\psi_1(\varepsilon, T) - \psi_3(\varepsilon, T)] \\
&+ \beta_2[\psi_2(\varepsilon, T) - \psi_3(\varepsilon, T)] + \psi_3(\varepsilon, T)\} + \bar{J}(\beta_1, \beta_2)
\end{aligned} \tag{28}$$

where $\bar{J}(\beta_1, \beta_2)$ is the indicator function of the triangle defined in the $\beta_1\beta_2$-plane as

$$\tau = \{(\beta_1, \beta_2) \,|\, 0 \le \beta_i \le 1;\ \beta_1 + \beta_2 \le 1\} \tag{29}$$

Now, from equations (4) and (5), considering that the pseudo-potential of dissipation does not depend on the strain rate, i.e., $\phi = \phi(\dot{\beta}_1, \dot{\beta}_2)$, one obtains

$$\sigma = C : \varepsilon + (\beta_2 - \beta_1)\,\alpha(T)\,I \tag{30}$$

and

$$\begin{aligned}
\frac{\partial\phi}{\partial\dot{\beta}_1} &= \alpha(T)\,\mathrm{tr}(\varepsilon) - \frac{L}{T_M}(T - T_M) - \partial_1\bar{J} \\
\frac{\partial\phi}{\partial\dot{\beta}_2} &= -\alpha(T)\,\mathrm{tr}(\varepsilon) - \frac{L}{T_M}(T - T_M) - \partial_2\bar{J}
\end{aligned} \tag{31}$$

where I is the identity tensor, while $\partial_1\bar{J}$ (resp. $\partial_2\bar{J}$) represents the subdifferential (Rockafellar, 1970) of the indicator function $\bar{J}(\beta_1, \beta_2)$ with respect to β_1 (resp. β_2).

The concepts of indicator function and subdifferential, are employed by Fremond in order to guarantee that β_1 and β_2 will be, at all time, inside or on the surface of the triangular region defined by equation (29). The use of Lagrange multipliers offers an alternative approach, which is also more suitable for numerical calculations based on this theory. The constraints to be satisfied are

$$-\beta_1 \le 0, \ -\beta_2 \le 0, \text{ and } \beta_1 + \beta_2 - 1 \le 0 \tag{32}$$

The indicator function may be written in the form

$$\bar{J} = -\lambda_1\beta_1 - \lambda_2\beta_2 + \lambda_3(\beta_1 + \beta_2 - 1) \tag{33}$$

from what follows

$$\frac{\partial \phi}{\partial \dot{\beta}_2} = -\alpha(T)\,\mathrm{tr}(\varepsilon) - \frac{L}{T_M}(T - T_M) + \lambda_2 - \lambda_3 \tag{34}$$

where λ_1, λ_2, and λ_3 are the Lagrange multipliers.

We also have to introduce a set of Kuhn-Tucker conditions (Luenberger, 1973):

$$\beta_1\lambda_1 = 0,\ \beta_2\lambda_2 = 0,\ \text{and}\ (\beta_1 + \beta_2 - 1)\lambda_3 = 0 \tag{35}$$

and

$$\lambda_1 \geq 0,\ \lambda_2 \geq 0,\ \text{and}\ \lambda_3 \geq 0 \tag{36}$$

Equations (30), (32), and (34-36), form the mathematical structure of the model with internal restrictions introduced by Fremond. An algorithm for the solution of this set of equations has been proposed by the authors (Savi and Braga, 1993).

It is worthwhile to compare Fremond's theory with that developed by Tanaka and presented elsewhere in this paper. In order to do so, we reduce Fremond's model to one-dimension, replacing the tensor ε and its trace by the uniaxial strain ε. Also, we use the component σ instead of the stress tensor σ, while the elasticity tensor **C** is replaced by the modulus E.

The most striking difference between the two models is that, while the theory developed by Fremond uses two kinds of martensite, Tanaka's considers only one. The first martensite in Fremond's model, β_1, is active only when the stress is positive (Fremond, 1987). Thus, keeping the comparison within tensile behavior at constant temperature, we observe that the constitutive equations (15) and (30) become very similar. In fact, the material parameter α has the same meaning in both models. Another point of contrast between these two theories, is the number of characteristic temperatures considered. Fremond assumes that both the martensitic and reverse transformations begin at $T=T_M$. Tanaka considers two different temperatures, T_M and T_A. The latter is associated with the start of the reverse transformation (martensite → austenite).

Despite these differences, it may be shown that both models predict identical response for successive tensile loading and unloading if we make the following assumptions: 1) the coefficients a_M, b_M, a_A, and b_A, become very large, approaching infinity in such a way that $a_A/b_A = a_M/b_M \rightarrow EL/\alpha T_M$; and 2) $T_A/T_M = 1+(\alpha^2/EL)$. The first assumption means that the transformation occurs instantaneously when the stress reaches the transformation line. The second is made in order to adjust the stress threshold for the reverse transformation. Plots showing the loading unloading paths predicted by both theories under these assumptions are presented in Fig. 4.

Finally, a few comments on the shortcomings of Fremond's three-dimensional model are in order. Firstly, it should be pointed out that, since the difference between the volumetric fractions of martensite variants appears multiplied by the identity tensor in Eq. (30), the model can not describe thermoelastic martensitic transformations induced by pure shear stress states. Results of torsion tests presented by Jackson et al. (1972) indicate, however, that these transformations do occur in nickel-titanium alloys.

A second remark, concerns the form assumed by Fremond's three-dimensional model when the stress-state is one-dimensional. In this case, if all three phases are assumed to behave isotropically, the trace of the strain tensor will also include a term proportional to the difference $(\beta_2-\beta_1)$. A more detailed analysis, out of the scope of the present contribution, will show that the resulting equations predict qualitatively different uniaxial stress-strain curves from those obtained experimentally, or by the other two one-dimensional models discussed in this article. This apparent shortcoming may be easily overcome by including another term in the expression of the free-energy.

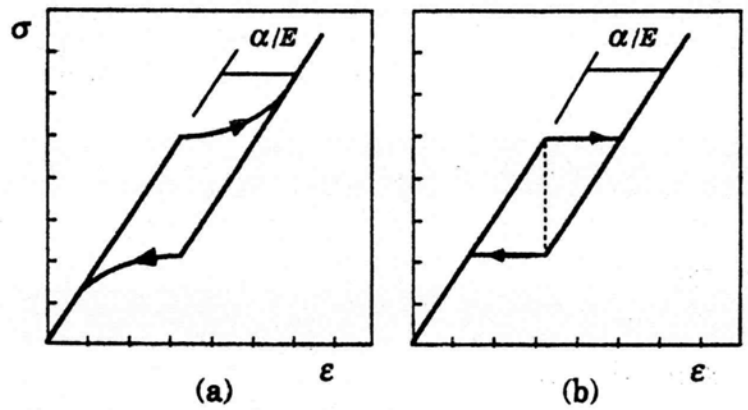

Fig. 4 Stress-strain curves at $T > T_A$: (a) predicted by Tanaka's model with exponential law; (b) obtained from both theories when assuming $a_A/b_A = a_M/b_M \rightarrow EL/\alpha T_M$ and $T_A/T_M = 1 + (\alpha^2/EL)$

An Helical Spring with Shape Memory

In order to model the response of an helical spring made from a shape memory alloy, one could apply any of the constitutive theories discussed in the preceding section. In fact, all three provide fairly good qualitative description of the one-dimensional shape memory and pseudoelastic effects. Here, we have chosen the polynomial free-energy function of Devonshire's theory. This choice yields the simplest equation for the nonlinear restoring force.

We assume that the longitudinal external force is resisted by the torsional shear stresses developed on the circular cross section of the helical shaped wire (Shigley, 1972; Tobushi and Sato, 1990). The relationship between the longitudinal force, F, and the shear stress distribution, σ, is expressed as

$$F = \frac{4\pi}{D}\int_0^{d/2} \sigma r^2 dr \tag{37}$$

where r is the radial coordinate along the cross-section, while D and d represent, respectively, the diameters of the spring and of the wire cross-section (Fig. 5).

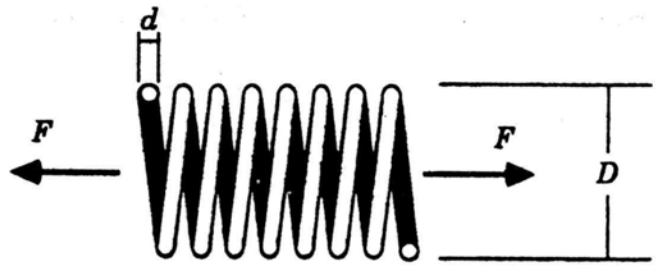

Fig. 5 Helical spring

We also assume that the shear strain, ε, is distributed linearly along the wire cross-section. If N is the number of coils and X the deflection, it can be shown (Shigley, 1972) that

$$\varepsilon = \frac{2r}{\pi D^2 N} X \tag{38}$$

Now, using the polynomial model, and assuming that Eq. (13) is valid for the pure shear stress-strain behavior, we obtain the following nondimensional equation for the nonlinear restoring force:

$$f = (\theta - 1)x - \lambda x^3 + \frac{\lambda^2}{4(\theta_C - 1)} x^5 \tag{39}$$

where f and x are the nondimensional force and displacement:

$$f = \frac{8D}{\pi a T_M d^3} F, \quad x = \frac{d}{\pi D^2 N} X \tag{40}$$

while the other parameters are defined as

$$\theta = \frac{T}{T_{M}}, \quad \lambda = \frac{2b}{3aT_M}, \text{ and } \theta_C = \frac{1}{9}\left(8\frac{T_A}{T_{M}} + 1\right) \tag{41}$$

The Oscillator with Shape Memory

We consider the one degree-of-freedom oscillator shown in Fig. 6. It consists of a mass m

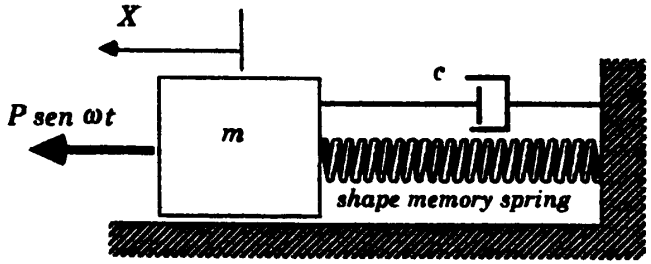

Fig 6. Oscillator with shape memory

supported by a shape memory spring and a linear damper with coefficient c. The system is excited harmonically by the force Psinωt. The nonlinear equation governing the forced motions of the oscillator may be written in the nondimensional form

$$\ddot{x} + \xi\dot{x} + (\theta - 1)x - \lambda x^3 + \frac{\lambda^2}{4(\theta_C - 1)} x^5 = \gamma \sin\Omega\tau \tag{42}$$

The dots represent derivatives with respect to the nondimensional time, τ, defined as

$$\tau = \omega_0 t, \text{ where } \omega_0 = \sqrt{aT_M d^4 / 8mD^3 N} \tag{43}$$

The other constants appearing in Eq. (42) are

$$\xi = c/m\omega_0, \quad \gamma = \frac{8D}{\pi a T_M d^3} P, \text{ and } \Omega = \omega/\omega_0 \tag{44}$$

If we define

$$y_1 = x \text{ and } y_2 = \dot{x} \tag{45}$$

Eq. (42) can be written as a first-order system:

$$\dot{y}_1 = y_2$$

$$\dot{y}_2 = -\xi y_2 - (\theta - 1) y_1 + \lambda y_1^3 - \frac{\lambda^2}{4(\theta_C - 1)} y_1^5 + \gamma \sin\Omega\tau \tag{46}$$

Free Vibrations

Free vibrations of the shape memory oscillator are described by the autonomous system obtained by letting γ vanish in Eqs. (46). In this section, we discuss the system response when it is displaced from an equilibrium configuration.

The fixed points, or equilibrium configurations, depend on the temperature. Denoting by $(\bar{y}_1, \bar{y}_2)$ a point in the y_1y_2-plane (the phase space) that, for γ=0, make the right-hand sides of Eqs. (46) vanish, we find five possibilities:

$$\bar{y}_1 = 0 \text{ and } \bar{y}_2 = 0 \tag{47}$$

or

$$\bar{y}_1 = \pm\left(\frac{2(\theta_C - 1)}{\lambda}\left(1 \pm \left(\frac{\theta_C - \theta}{\theta_C - 1}\right)^{1/2}\right)\right)^{1/2} \text{ and } \bar{y}_2 = 0 \tag{48}$$

Of these five possibilities, only those which correspond to real numbers have physical meaning. Hence,

a) for $\theta \le 1$, the system has three fixed points;

b) for $1 < \theta < \theta_C$, the system has five fixed points;

c) for $\theta = \theta_C$, the system has three fixed points;

d) for $\theta > \theta_C$, the system has only one fixed point.

Stability of these equilibrium configurations are determined by the behavior of the linearized system in their neighborhood. By making the change of variables

$$\eta_j = y_j - \bar{y}_j \quad (j = 1, 2) \tag{49}$$

and considering η_j small, the autonomous (γ=0) linearized system assumes the form

$$\dot{\eta}_1 = \eta_2$$

$$\dot{\eta}_2 = -\left((\theta - 1) - 3\lambda\bar{y}_1^2 + \frac{5\lambda^2}{4(\theta_C - 1)}\bar{y}_1^4\right)\eta_1 - \xi\eta_2 \tag{50}$$

An analysis of the eigenvalues of this system reveals that, for $\theta \le 1$, the origin of the phase space, which corresponds to a state of rest, is a saddle point. The other two fixed points are centers when ξ=0 (undamped system) or stable spirals when $\xi > 0$. This is consistent with the low temperature behavior of the shape memory alloy, where two martensitic phases are stable.

When $1 < \theta < \theta_C$, the system has two saddle points in the phase space. These are

$$\bar{y}_1 = \pm\left(\frac{2(\theta_C - 1)}{\lambda}\left(1 - \left(\frac{\theta_C - \theta}{\theta_C - 1}\right)^{1/2}\right)\right)^{1/2} \text{ and } \bar{y}_2 = 0 \tag{51}$$

The remaining three fixed points are centers if the system has no dissipation. They are stable spirals otherwise. The existence of three stable fixed points is explained by the stability of both martensitic phases and the parent austenite in this temperature range.

When $\theta = \theta_C$, the origin is a center if ξ=0, or a stable spiral if the system is dissipative. The other two fixed points are saddles. Finally, for $\theta > \theta_C$, the origin, which now is the only stable fixed point in the phase plane, is either a center or a spiral, again depending whether the system is dissipative or not. For $\theta > \theta_C$, austenite is the only stable phase in the stress-free shape memory alloy.

Fig. 7 shows some phase plane trajectories illustrating the free vibration of the undamped shape memory oscillator at three different temperatures. These results have been obtained by numerical integration of Eqs. (46). The standard fourth-order Runge-Kutta algorithm has been used in these calculations. We have obtained good convergence with a step size $\Delta\tau = 2\pi/180$. Since we are, at this

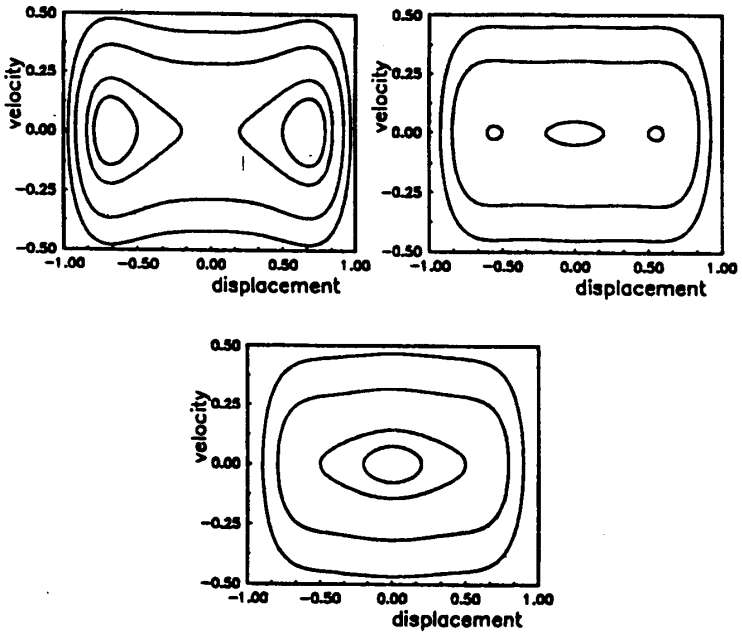

Fig. 7 Phase portraits of the unforced non dissipative system ($\xi = 0$).
(a) $\Theta < 1$; (b) $1 < \Theta < \Theta_c$; (c) $\Theta < \Theta_c$

point, more concerned with the qualitative response of the shape memory system, we have chosen λ=1 for the example calculations presented throughout this article. We have also assumed θ_C=1.10, which is a typical value for nickel-titanium alloys (Tobushi and Tanaka, 1990).

Results showing the phase plane trajectories for the dissipative system (ξ=0.2) at constant temperature are presented in Fig. 8. We observe that when the system has more than one dynamical attractor, which is the case when $\theta < \theta_C$ (Figs. 8a and 8b), its final configuration is very sensitive to the initial condition. This is a common feature of nonlinear systems.

Fig. 9 shows the behavior of the autonomous system subjected to a temperature variation. This result has been obtained by assuming that the temperature of the system, initially θ_i, changes to θ_f in the following way:

$$\theta = \begin{cases} \theta_i & \text{if} \quad \tau \le \tau_i; \\ \theta_i + (\theta_f - \theta_i)\sin\dfrac{\pi(\tau-\tau_i)}{2(\tau_f-\tau_i)} & \text{if } \tau_i < \tau < \tau_f; \\ \theta_f & \text{if} \quad \tau \ge \tau_f; \end{cases} \tag{52}$$

The mass is displaced from its equilibrium position at the instant τ=0. After an interval of time, τ_i, the temperature begins to change, up to the instant τ_f, when it reaches the final temperature level. In Fig. 9a, we have considered the undamped oscillator. The plot in Fig. 9b has been obtained for the dissipative system. The dashed line represents the transient behavior between τ_i and τ_f. As expected, the oscillator settles on a different attractor after the new temperature level is reached. This behavior is

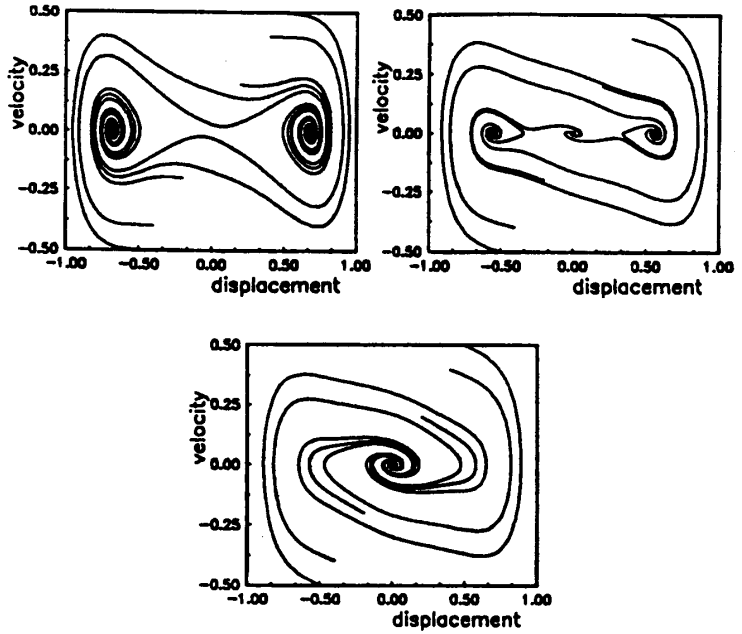

Fig. 8 Phase portraits of the unforced dissipative system ($\xi = 0.2$).
(a) $\Theta < 1$; (b) $1 < \Theta < \Theta_c$; (c) $\Theta < \Theta_c$

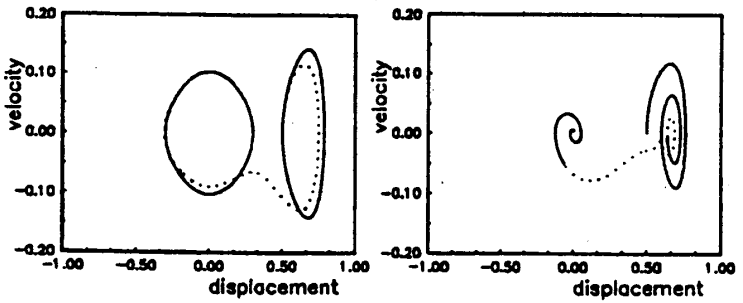

Fig. 9 Unforced system subjected to a temperature variation. $\theta_i = 0.95$; $\theta_f = 1.16$
(a) Non dissipative system ($\xi = 0$). (b) Dissipative system ($\xi = 0.2$).

of special interest, since it illustrates the capability of altering the dynamics of the shape memory system by changing its temperature. We shall return to this point when discussing the forced response of the oscillator.

Chaotic Vibrations of the Shape Memory Oscillator

The behavior of the forced system is far more complex. In this section, we discuss the response of the shape memory oscillator to periodic excitations. In particular, we are concerned with the prospect of chaotic behavior. The system is governed by Eqs. (46), where γ and Ω are the nondimensional parameters representing, respectively, the amplitude and frequency of the sinusoidal forcing function. For the numerical examples presented in this section, we have taken $\Omega=1$ and let γ vary.

Initially, we observe the response when the forcing amplitude is small. Fig. 10 shows results of the

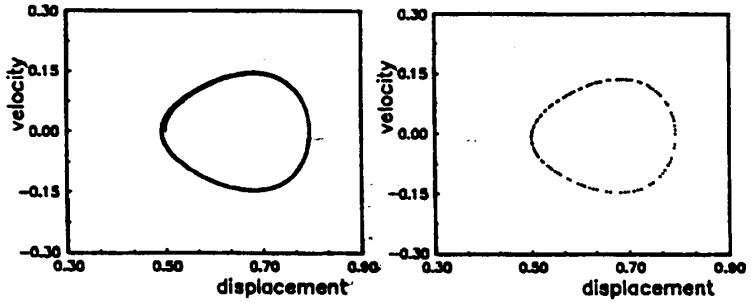

Fig. 10 Quasi-periodic response of the system. $\xi = 0$; $\theta = 0.95$; $\gamma = 10^{-3}$
(a) Phase plane trajectory; (b) Poincaré section of the orbit

numerical integration when $\xi=0$, $\theta=0.95$ and $\gamma=10^{-3}$. Along with the phase plane trajectory in Fig. 10a, we also show a Poincaré section of the orbit, which is obtained by sampling the state variables, displacement and velocity of the oscillator, at a rate equal to the forcing period. This procedure may be better understood if we view the forced oscillator as an autonomous system with a three-dimensional phase space. Time, in fact the quantity $\Omega\tau$, is taken here as the third explicit state variable. Also, since the forcing is periodic, one considers the state space as the Cartesian product of the Euclidian 2-space, the plane, with the circle (see, e.g., Guckenheimer and Holmes, 1983, pp. 25-27). The set of points on the Poincaré section are then the intersections of the orbit with a plane that cuts this cylindrical state space at $\Omega\tau=\varphi$, where φ is a constant between 0 and 2π. Discussions on this geometrical view of dynamical systems may be found, for instance, in (Abraham and Shaw, 1982; Wiggins, 1988; Wiggins, 1990).

The phase plane trajectory shown in Fig. 10a, indicates that the system oscillates around one of the equilibrium configurations associated with this temperature and initial conditions. The Poincaré section in Fig. 10b, reveals that the motion is in fact quasi-periodic. A periodic orbit is shown in Fig. 11. Now, we have taken $\theta=0.95$, $\xi=0.2$, and $\gamma=0.05$. In this case, the Poincaré section is simply a point in the phase plane.

As the forcing parameter γ increases, the system dynamics becomes reacher. Fig. 12 shows the time history of the oscillation amplitude when $\theta=0.95$ and $\gamma=5$. The plot in Fig. 12a has been obtained for $\xi=0$, while in Fig. 12b we have taken $\xi=0.1$. In both cases, the system response shows no visible periodicity. The Poincaré section for the undamped system, displayed in Fig. 13a, now consists of a cloud of points that fills the phase plane with no noticeable structure. This lack of structure is common in nondissipative chaos.

Although the time history of the dissipative system is very similar to that of the undamped oscillator (Figs. 12a and 12b), its Poincaré section, shown in Fig. 13b, appears as a set of points arranged in a highly organized fashion. Poincaré sections illustrating the forced response of the damped oscillator at different temperatures are shown in Fig. 14. All plots show the same fractal-like structure. In fact, such structured collections of points correspond to Cantor Sets (see, e.g., Guckeinheimer and Holmes, 1983; Thompson and Stewart, 1986; Moon, 1987; Wiggins, 1988;

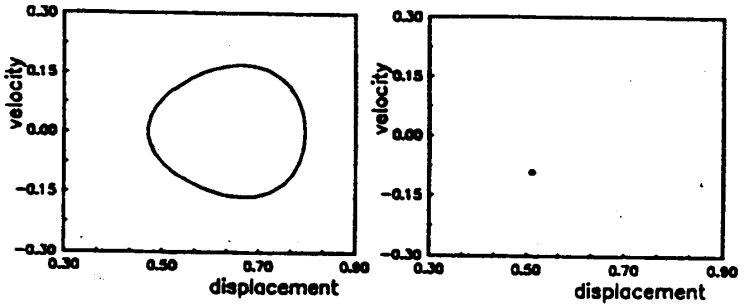

Fig. 11 Periodic response of the system. $\xi = 0.2$; $\theta = 0.95$; $\gamma = 0.05$
(a) Phase plane trajectory; (b) Poincaré section of the orbit

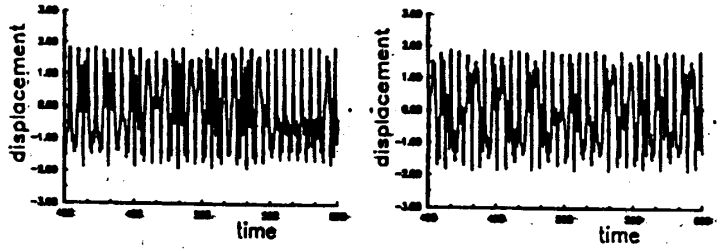

Fig. 12 Time history of a chaotic response. $\xi = 0$; $\theta = 0.69$; $\gamma = 5$
(a) Non dissipative system ($\xi = 0$); (b) Dissipative system ($\xi = 0.1$)

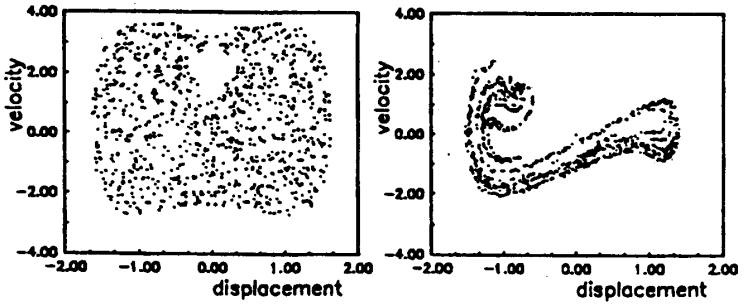

Fig. 13 Poincaré section of a chaotic response. $\theta = 0.69$; $\gamma = 5$
(a) Non dissipative system ($\xi = 0$); (b) Dissipative system ($\xi = 0.1$)

Wiggins, 1990), and are indication of the folding and stretching experienced by the chaotic orbits of the forced, damped oscillator. These collections of points are called strange attractors (Moon, 1987), and are usually found in dissipative chaos.

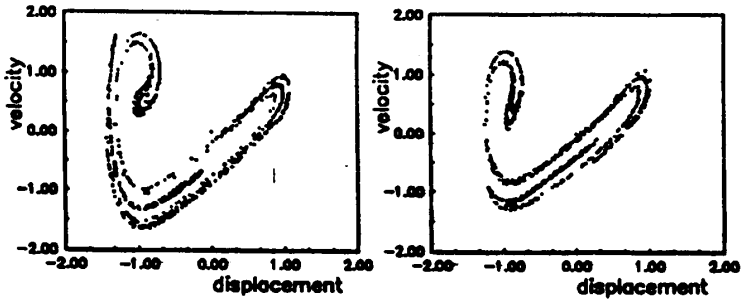

Fig. 14 Poincaré section of a chaotic response in a dissipative system ($\xi = 0.2$) at different temperatures. (a) $1 < \theta < \theta_c$; $\gamma = 5$; (b) $\theta > \theta_c$; $\gamma = 4.5$

The fractal set on the Poincaré section is in fact a cross section of the three-dimensional attracting structure embedded in the cylindrical phase space. It is interesting to observe the evolution of orbits initiated at a circle of states (initial displacement and velocity) on the phase plane. After successive time intervals, we check the intersections of this set of orbits with the phase plane. This is shown in Fig. 15. If the attracting orbit is periodic, the circle of initial states is mapped to a point (Fig. 15a). When the response is chaotic, the original circle is continuously stretched and folded approaching a fractal-like structure (Fig. 15b). This picture, which is a common feature of chaotic motions, corresponds to the so-called Smale horse-shoe (Wiggins, 1988). Another view of the attracting structure is presented in Fig. 16, that shows Poincaré sections taken at different values of $\Omega\tau$.

A bifurcation diagram is presented in Fig. 17, demonstrating the influence of the driving amplitude on the system dynamics. It is interesting to notice the presence of periodic windows, and the occurrence of a cascade of period doubling bifurcations leading to chaos in one of these windows (enlarged region in the upper right corner of the figure). The pattern in Fig. 17 is typical of a number of nonlinear dynamical system that exhibit chaotic behavior (Grebogi et al., 1983).

Finally, Fig. 18 shows a transition from chaotic to periodic response due to a variation in the system temperature. This plot, again illustrates the capability of altering the dynamics of the shape memory oscillator with the temperature. This feature has motivated the use of shape memory alloys as actuators for active vibration control of structures responding in the linear range (Rogers, 1990; Rogers et al., 1991; Venkatesh et al., 1992). It should be pointed out, however, that in these applications the actuators have been employed under conditions where the SMA stress-strain behavior could be linearized.

Concluding Remarks

In this paper, we have focused on the qualitative behavior of a simple dynamical system with shape memory. Three different theories that model the phase transformations associated with pseudoelasticity and the shape memory effect have been reviewed. All three theories provide satisfactory qualitative one-dimensional description of these effects. Only one of these models, however, can be applied to three-dimensional stress states.

The constitutive theory that assumes a polynomial expression for the free-energy functional has been used to model an helical spring with shape memory. This choice yields the simplest analytical form for the nonlinear restoring force. The dynamics of an one degree-of-freedom oscillator containing such a spring has been studied numerically.

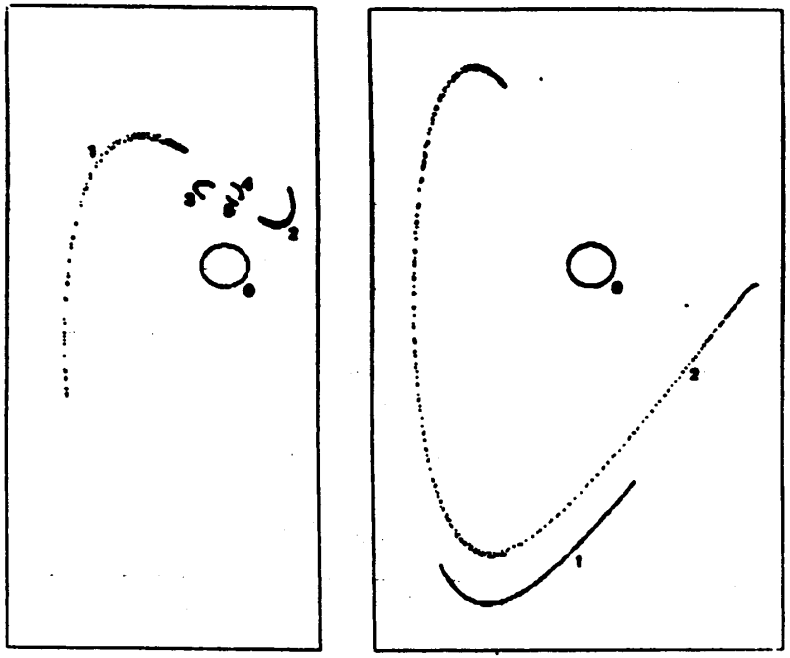

Fig. 15 Evolution of a ball of initial conditions in the phase space (a) Periodic motion; (b) Chaotic motion

Results of the numerical simulations indicate that this mechanical oscillator may exhibit chaotic response under certain conditions. Despite the limitations of the analytical model used here, and the lack of experimental data, the authors believe that similar behavior may be expected in other systems with shape memory. This conclusion suggests that the possibility of chaotic response should be considered when designing shape memory actuators for vibration and structural acoustic control.

Acknowledgements

The authors would like to thank Prof. H. Costa Mattos fo his insightful comments on the constitutive modeling of shape memory. During the course of this work, M. A. Savi has been supported by a grant from CNPq. Support from the Brazilian Ministry of Science and Technology to PUC-Rio is also gratefully acknowledged.

References

Abraham, R. H. and Shaw, C. D., 1982, Dynamics - The Geometry of Behavior, Parts 1-3, Aerial Press, Santa Cruz, California.

Achenbach, M. and Müller, I., 1982, "A Model for Shape Memory", J. de Physique, Colloque C4, Suppl. 12, Tome 43, pp. 163-167.

Buekler, W. J., Gilfrich, J. V. and Wiley, R. C., 1963, "Effect of Low-Temperature Phase Changes on The Mechanical Properties of Alloys Near Composition TiNi, "J. Appl. Phys., Vol. 34, pp. 1475-1477.

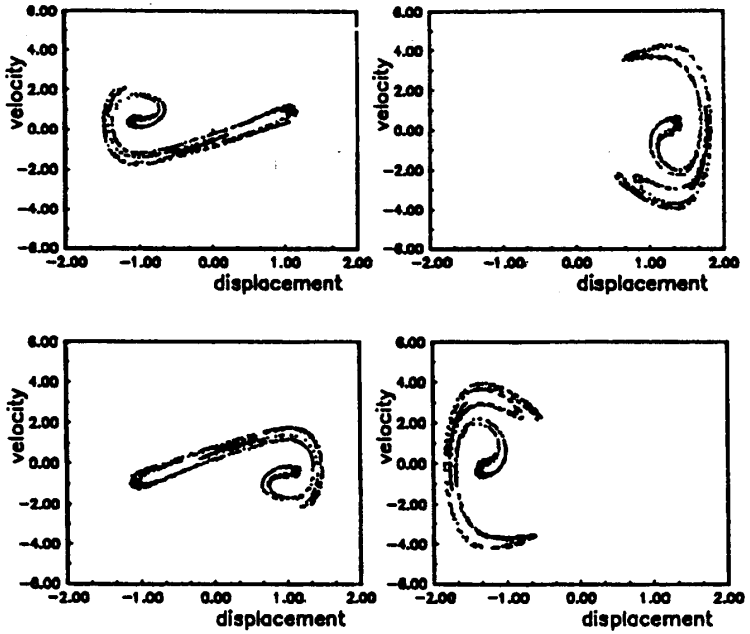

Fig. 16 Evolution of the chaotic attractor for different positions of the Poincaré section.

$\theta = 0.69$; $\xi = 5$ (a) $\varphi = 0$; (b) $\varphi = \pi/2$; (c) $\varphi = \pi$; (d) $\varphi = 3\pi/2$

Delaey, L., Krishnan, R.V., Tas, H. and Warlimont, H., 1974, "Thermoelasticity, Pseudoelasticity and The Memory Effects Associated with Martensitic Transformations, Part 1: Structural and Microstructural Changes Associated with the Transformations", J. Mat. Sci., Vol. 9, pp. 1521-1535.

Falk, F., 1982, "Landau Theory and Martensitic Phase Transitions", J. de Physique, Colloque C4, Suppl. 12, Tome 43, pp. 3-15.

Fremond, M., 1987, "Matériaux à Mémoire de Forme", C. R. Acad. Sc. Paris, Tome 304, s.II, No. 7, pp. 239-244.

Germain, P., 1973, Mécanique des Millieux Continus, Dunod, Paris.

Grebogi, C., Ott, E. and Yorke, J. A., 1983, "Crises, Sudden Changes in Chaotic Attractors, and Transient Chaos", Physica 7D, pp. 181-200.

Guckenheimer, J. and Holmes, P., 1983, Nonlinear Oscillations, Dynamical Systems, and Bifurcations of Vector Fields, Springer-Verlag, New York.

Jackson, C. M., Wagner, H. J. and Wasilewski, R. J., 1972, 55-Nitinol - The Alloy with a Memory: Its Physical Metallurgy, Properties, and Applications, NASA-SP-5110.

Liang, C. and Rogers, C. A., 1990, "A One-Dimensional Thermomechanical Constitutive Relation of Shape Memory Materials", Proceedings of the 31st Structure, Structural Dynamics and Materials Conference, paper AIAA-90-1027, Long Beach, CA, AIAA, pp. 2234-2241.

Luenberger, D. G., 1973, Introduction to Linear and Nonlinear Programming, Addison-Wesley, Reading, New Jersey.

Moon, F. C., 1987, Chaotic Vibrations, Wiley-Interscience, New York.

Rockafellar, R. T., 1970, Convex Analysis, Princeton Press, New Jersey.

Rogers, C. A., 1990, "Active Vibration and Structural Acoustic Control of Shape Memory Alloy Hybrid Composites: Experiemental Results", J. Acoust. Soc. of Am., Vol. 88, pp. 2803-2811.

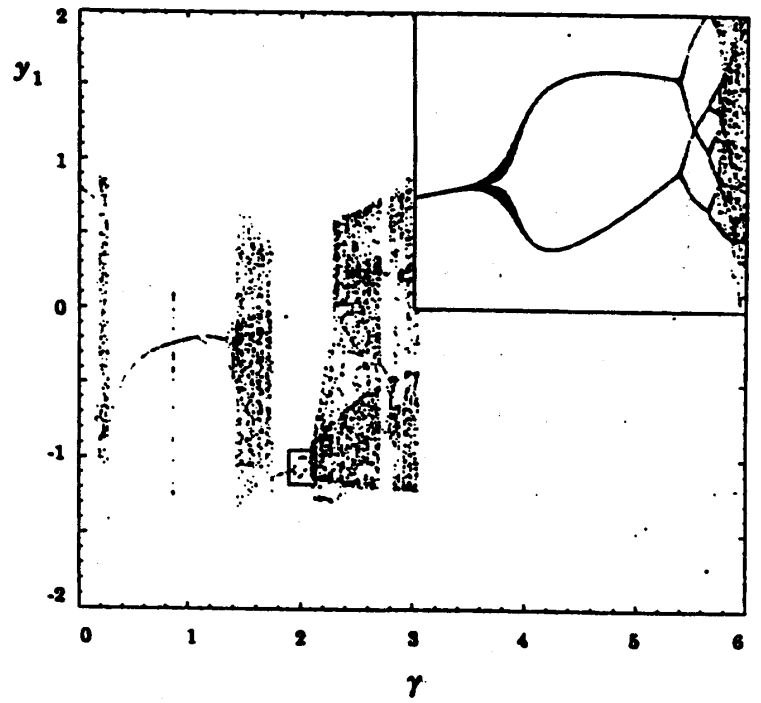

Fig. 17 Bifurcation diagram ($\xi = 0.2$, $\Omega = 1$

Rogers, C. A., Liang, C., and Jia, J., 1989, "Behavior of Shape Memory Alloys Reinforced Composite Plates, Part 1: Model, Formulation and Control Concepts", Proceeding of the 30th Structure, Structural Dynamics and Materials Conference, paper AIAA-89-1389, Mobile, AL, AIAA, pp. 2011-2017.

Rogers, C. A., Liang, C. and Fuller, C. R., 1991, "Modeling of Shape Memory Alloy Hybrid Composites for Structural Acoustic Control", J. Acoust. Soc. of Am., Vol. 89, pp. 210-220.

Sato, Y., Tanaka, K. and Kobayashi, S., 1985, "Pseudoelasticity and Shape Memory Effect Associated with Stress-Induced Martensitic Transformation: A Thermomechanical Approach", Trans. Japan Soc. Aero. Space Sci., Vol. 28, No. 81, pp. 150-160.

Savi, M. A. and Braga, A. M. B., 1993, "Chaotic Response of a Shape Memory Oscillator with Internal Constraints", accepted for publication in: Proceeding of the 12th. Brazilian Congress of Mechanical Engineering.

Schetky, L. M., 1979, "Shape Memory Alloys", Sci. Am., Vol. 241(5), pp. 68-76.

Shigley, J. E., 1972, Mechanical Engineering Design, 2nd. ed., McGraw-Hill Kogagusha, Tokyo.

Tanaka, K., 1985, "A Thermomechanical Sketch of Shape Memory Effect: One-Dimensional Tensile Behavior", Res. Mech., Vol. 18, p. 251.

Tanaka, K. and Nagaki, S., "A Thermomechanical Description of Materials with Internal Variables in the Process of Phase Transitions", Ing. Arch., Vol. 51, pp. 287-299.

Thompson, J. M. T. and Stewart, H. B., 1986, Nonlinear Dynamics and Chaos, John Willey and Sons, Chichester, England.

Tobushi, H. and TANAKA, K., 1990, "Deformation of a Shape Memory Alloy Helical Spring", JSME Int. J., Ser. I, Vol. 34(1), pp. 83-89.

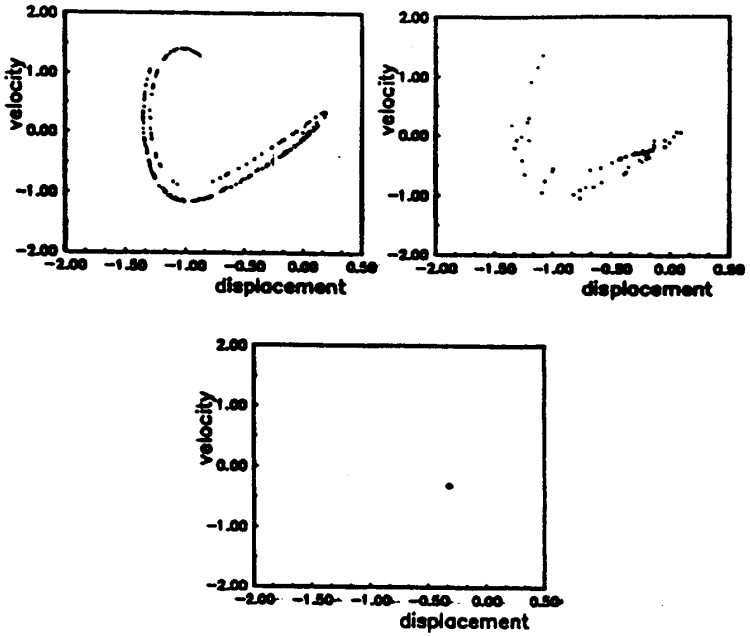

Fig. 18 Transition from chaotic to periodic response due to a variation in the system temperature $\theta_i = 0.69$; $\theta_f = 2.08$; $\xi = 0.5$; (a) Chaotic response at constant temperature (b) Transient response; (c) Periodic response at the new temperature

Venkatesh, A., Hilborn, J., Bidaux, J. E. and Gotthard, R., 1992, "Active Vibration Control of Flexible Linkage Mechanism Using Shape Memory Alloy Fiber Reinforced Composites", Proceedings of the 1st European Conference on Smart Structures and Materials, Glasgow, Scotland, IOP Publishing, pp. 185-188.

Warlimont, H., Delaey, L., Krishnan, R. V. and Tas, H., 1974, "Thermoelasticity, Pseudoelasticity and The Memory Effects Associated with Martensitic Transformations, Part 3: Thermodynamics and Kinetics", J. Mat. Sci., Vol. 9, pp. 1545-1555.

Wiggins, S., 1988, Global Bifurcations and Chaos, Springer-Verlag, New York.

Wiggins, S., 1990, Introduction to Applied Nonlinear Dynamical Systems and Chaos, Springer-Verlag, New York.